

# Straight GDP-tubulin protofilaments form in the presence of taxol.

Céline Elie-Caille<sup>1,2</sup>, Fedor Severin<sup>1</sup>, Jonne Helenius<sup>1</sup>, Jonathon Howard<sup>3</sup>, Daniel J.

Muller<sup>1\*</sup>, A.A Hyman<sup>3\*</sup>

<sup>1</sup> Dept. Cellular Machines, BioTechnological Center, University of Technology Dresden, Tatzberg 49, D-01307 Dresden, Germany.

<sup>2</sup> FEMTO-ST Institute, UMR6174-CNRS, Department of Physics and Metrology of Oscillators, 32 avenue de l'observatoire, 25044 Besançon Cedex, France.

<sup>3</sup> Max Planck Institute of Molecular Cell Biology and Genetics, Pfotenhauer Str. 108, D-01307 Dresden, Germany.

**Running title:** Conformational transitions of microtubule protofilaments

**Number of words:** 1780

**Abbreviations:** AFM, atomic force microscopy; GMPCPP, guanylyl ( $\alpha,\beta$ )methylenediphosphonate.

\* Address correspondence to

DJM at [mueller@biotec.tu-dresden.de](mailto:mueller@biotec.tu-dresden.de) and AAH at [hyman@mpi-cbg.de](mailto:hyman@mpi-cbg.de)

**SUMMARY**

Microtubules exist in dynamic equilibrium, growing and shrinking by addition or loss of tubulin dimers from the ends of protofilaments. Hydrolysis of GTP in  $\beta$ -tubulin destabilizes the microtubule lattice by increasing the curvature of protofilaments in the microtubule and putting strain on the lattice. The observations that protofilament curvature depends on GTP hydrolysis suggest that microtubule destabilizers and stabilizers work by modulating the curvature of the microtubule lattice itself. Indeed, the microtubule destabilizer MCAK has been shown to increase the curvature of protofilaments during depolymerization. Here we show that atomic force microscopy (AFM) of individual tubulin protofilaments provides sufficient resolution to allow imaging of single protofilaments in their native environment. Using this assay we confirm previous results for the effects of GTP hydrolysis and MCAK on the conformation of protofilaments. We go on to show that taxol stabilizes microtubules by straightening the GDP protofilament, and slowing down the transition of protofilaments from straight to a curved configuration.

## RESULTS AND DISCUSSION.

### **The curvature of individual protofilaments can be assayed by AFM.**

To look at the structure of individual protofilaments by AFM<sup>1,2</sup>, we used calcium to depolymerize microtubules polymerized with GMPCPP<sup>3</sup>. The depolymerization products of GMPCPP microtubules were adsorbed to mica and imaged using tapping mode AFM in buffer (Fig.1A). Numerous curled single protofilaments were observed with a curvature of  $31 \pm 5$  nm, close to the curvature of  $36 \pm 10$  nm measured previously using vitreous ice<sup>3</sup>. These previous experiments showed that GMPCPP is not hydrolyzed under these conditions<sup>3</sup>; they also showed that depolymerization of microtubules either by cooling or by calcium addition generated protofilaments with the same curvature. Therefore GMPCPP protofilaments depolymerized with calcium are thought to represent the structure of GTP protofilaments<sup>3,4</sup>. We compared the curvature of GMPCPP protofilaments to those of GDP protofilaments (Fig.1B). Protofilaments present during normal polymerization have radii of  $21 \pm 4$  nm ( $n=45$ ) and protofilaments from calcium induced depolymerization of  $21 \pm 2$  nm ( $n=56$ ) (Table 1), again confirming the results of cryo-EM ( $21.1 \pm 4.3$  nm)<sup>3</sup>. Therefore we conclude that AFM allows the analysis of the conformation of protofilaments under native conditions.

### **Taxol slows the straight-to-curved transition of GDP protofilaments.**

We next examined the effect of taxol on the configuration of protofilaments. Taxol does not inhibit the hydrolysis of microtubule-bound GTP<sup>5</sup>, but slows down microtubule depolymerization<sup>6</sup>. Cryo-EM observations show that as with GMPCPP, taxol increases the length of tubulin monomers in microtubules from 4.01 to 4.17 nm<sup>7</sup>.

This suggests that taxol could stabilize microtubules by preventing the protofilaments from curving and putting mechanical strain on the tubulin lattice. The small change in the size of the subunit would correspond to the decreased length associated with bending of the subunit.

Using AFM, we showed that microtubules polymerized with taxol contained a significant number of individual protofilaments (Fig.1C). To exclude the possibility that the supporting surface induced formation of protofilaments, we showed that AFM topographs of glutaraldehyde fixed microtubules contained similar amounts and appearance of protofilaments compared to unfixed ones (data not shown). Thus our data are consistent with previous observations that individual protofilaments coexist with microtubules in freshly prepared taxol-stabilized microtubule samples<sup>8</sup>.

Taxol-stabilized protofilaments were mainly straight or slightly curved, but occasionally formed rings (Fig.1C). The radius of curvature of slightly curved protofilaments was  $245 \pm 105$  nm ( $n=51$ ), (compared to  $31 \pm 5$  nm for GMPCPP protofilaments (Table 1)). The radius of closed rings (cf Fig.1D) was  $21 \pm 2$  nm ( $n=48$ ), similar to the radius of GDP protofilament rings. To test whether the slightly curved taxol protofilaments represented transition states between straight and protofilaments rings, we examined the structure of protofilaments with time after polymerization. We prepared taxol-stabilized microtubules and imaged them by AFM 1, 4, 6, 7, 24 and 50 hours after polymerization (Fig.2). These topographs show that straight protofilaments are very stable- up to four hours, most of taxol protofilaments are straight. The most likely explanation for these data is that taxol initially stabilizes protofilaments in a straight conformation. Because

GTP is hydrolysed in taxol-stabilized microtubules<sup>9</sup>, these data suggest that taxol actively straightens protofilaments. The majority of the protofilaments are in a straight configuration up to six hours after preparation. Given the time scale of microtubule life time during polymerization (minutes) it is likely that the protofilaments remain straight when taxol stabilizes microtubules. However at longer time scales, the protofilaments slowly convert to the curved conformation, and by 24 hours they eventually close up into rings, reminiscent of the structure of GDP protofilaments. How does taxol slow down the straight to curled transition of GDP protofilaments? One likely possibility is that taxol slows down the intrinsic structural transition from straight to curved that takes place in GDP protofilaments. However we cannot rule out that taxol itself is slowly inactivated in an aqueous environment.

Van Buren et al (2005)<sup>10</sup> proposed that taxol might stabilize microtubules by making the protofilaments less stiff rather than making them less curved: in both cases the mechanical strain energy penalty for tubulin in the microtubule lattice is reduced. We have no evidence indicating that taxol does not soften protofilaments because our AFM images provide no information about protofilament rigidity; however, we note that it is not established that taxol even has a softening effect on microtubules - see e.g. Mickey, B. and Howard, J.<sup>11</sup> who found that taxol actually increased slightly the flexural rigidity of GDP microtubules.

### **GTP hydrolysis and kink between tubulin monomers.**

Previous experiments suggest that protofilament curvature increases after GTP hydrolysis because tubulin subunits in the lattice shorten, changing the repeat length of the tubulin dimers from 4.20 to 4.05 nm<sup>12</sup>. This lead to the conclusion that a

conformational change within tubulin subunits induced by GTP hydrolysis induces protofilament curvature. Recent structural analysis of the two alternative tubulin structures, both straight and curved protofilaments at atomic resolution have shown that indeed, GTP hydrolysis induces a  $12^\circ$  kink between the tubulin subunits<sup>13</sup>. The kink angle was obtained by reconstructing cryo-EM images recorded from double-layered tubes of GDP bound tubulin<sup>4</sup>. Thus, it was not possible to directly compare these tubulin polymer conformations with those of protofilaments induced by various stabilizing and destabilizing factors and conditions. Using high-resolution AFM topographs we were able to distinguish individual tubulin subunits in the protofilaments (Fig.3). By averaging the tubulin distances contoured in the height profiles of 10 straight taxol-stabilized protofilaments such as shown in Fig.3A we obtained a periodicity of  $4.2 \pm 1.6$  nm ( $n=104$ ) (Fig.3B), corresponding well to the known size of monomeric tubulin, 4 nm<sup>14</sup>. Second, combining tubulin periodicity and protofilament radius of curvature allowed us to calculate the kink angle established between the tubulin subunits (see materials and methods).

We calculated the kink in GMPCPP-stabilized protofilaments and GDP protofilaments, and compared this to the published data from other methods. GMPCPP protofilaments form curled protofilaments with an average radius of curvature of  $31 \pm 5$  nm ( $n=35$ ) in presence of 40 mM  $\text{Ca}^{2+}$ . This gives a calculated value of  $7.8 \pm 1.2^\circ$  ( $n=63$ , 40 mM  $\text{Ca}^{2+}$ ) for the kink angle between dimers. This differs from the  $5^\circ$  kink found between subunits in tubulin sheets<sup>13</sup>. This difference may be because the kink of subunits within tubulin sheets is constrained<sup>15</sup>. The radius of GDP protofilament rings was  $21 \pm 2$  nm ( $n=56$ ) independently of whether 40 mM  $\text{Ca}^{2+}$  or MCAK was present in the sample

(Fig.3F). With 30 subunits to a ring (Fig.3D,E) the tubulin subunits within these protofilament had a kink of  $12^\circ$ , exactly that found between tubulin monomers of a GDP tubulin dimer in the relaxed, curved conformation<sup>13</sup>. Thus these data confirm that a change in the kink between tubulin subunits can account for the change in radius of curvature of the protofilaments.

Next, we calculated the time-dependent changes in the kink angle between the subunits in taxol-stabilized protofilaments (Fig.3F). 1 hour after preparation of taxol-stabilized protofilaments, tubulin monomers of protofilaments showed an average kink close to  $0^\circ$ , after 7 hours this kink increased slightly enhanced to  $\sim 1^\circ$ . However, after 24 hours all taxol-stabilized protofilaments were in rings, with a calculated kink angle of  $12^\circ$ . These results support previous analysis by Arnal and Wade (1995)<sup>7</sup> who looked at the periodicity of tubulin subunits in the lattice and showed that the most likely mechanism by which taxol stabilize microtubules is by preventing the GDP subunit adopting a kinked configuration after GTP hydrolysis.

### **MCAK increases the curvature of GTP protofilaments and kink between tubulin subunits.**

Previous EM results suggested that MCAK induces curvature in GTP-like protofilaments<sup>16</sup>. Based on these and other observations<sup>17,18</sup>, it has been suggested that the microtubule destabilizing factors, such as KLP-7, bend tubulin dimers thus destabilizes microtubules<sup>17,18</sup>. To further test this idea, MCAK was added to microtubules grown both in the presence of GMPCPP or GTP with taxol. AMPPNP was added to inhibit MCAK and to tightly bind it to microtubules<sup>17</sup>. After 5 min

incubation the resulting structures were imaged by AFM. The AFM topographs showed some “intact” microtubule ends and numerous ring-like protofilaments (Fig.1F,G). In contrast to the effects observed using only the MCAK motor core<sup>17</sup>, protofilaments obtained in the presence of the complete MCAK protein were predominantly single rings with a  $19 \pm 2$  nm ( $n=37$ ) radius of curvature while no double or triple concentric rings were observed. The protofilament radius from taxol-stabilized microtubules  $19 \pm 2$  nm (Fig.1G, Table 1), was similar to previously published EM data<sup>17</sup>. The radius of ring-like protofilaments from GMPCPP microtubules was  $27 \pm 4$  nm ( $n=43$ ) (Fig.1E, Table 1). From these data we calculated that MCAK increased the kink between tubulins from  $7.8 \pm 1.2^\circ$  ( $n=63$ , 40 mM  $\text{Ca}^{2+}$ ) to  $8.9 \pm 1.2^\circ$  ( $n=43$ ) (Table 1, Fig.3F). Thus, in agreement with Desai (1999)<sup>16</sup> and Moores<sup>17</sup> (2002), the AFM data indicate that MCAK bends tubulin protofilaments made of GTP tubulin. Interestingly, addition of MCAK to the sample of taxol-stabilized microtubules in the presence of ATP instead of AMPPNP did not induce formation of protofilament rings. We speculate that ATP hydrolysis and MCAK release from protofilaments occur more rapidly than protofilament bending. An alternative possibility is that the complete ATPase cycling allows disassembly of the protofilaments into tubulin dimers, suggesting that MCAK may induce a greater kink between tubulin monomers, increasing protofilament curvature.

The idea that microtubule stabilizers and destabilizers work through the curvature of protofilaments is a fascinating link between the global structural change of a microtubule and the small chemical change from GTP to GDP, within its tubulin dimers. By straightening the GDP protofilaments, taxol apparently prevents GTP

hydrolysis from putting strain on the microtubule lattice. In this context, it is interesting that taxol-stabilized protofilaments had radii either greater than 200 nm or around 20 nm, and both populations were found in the same samples. This indicates that kinking occurs simultaneously in the 20-30 dimers of a protofilament, suggesting a long-distance cooperative interaction between dimers of a protofilament. Cooperative kinking may act as a growth-to-shrinkage switch and explain why microtubules undergo catastrophic disassembly. It will be fascinating to see how other modulators of microtubule stability alter the conformation of the protofilaments.

Taxol is used as an anticancer agent<sup>19</sup>. Its action on microtubules suggests a mechanism by which arrest in mitosis is due to changes in microtubule stability that induce apoptosis of cancerous cells. Our data on the effect of taxol on the microtubule lattice suggest a potentially more complex explanation for the efficiency of taxol. By straightening the protofilaments, taxol induces a more GTP-like configuration in the protofilament. Since proteins can distinguish the GTP from the GDP configuration microtubule lattice<sup>20,21</sup>, perhaps putting the protofilaments into a GTP-like configuration triggers physiological changes in the apoptosis machinery that are different from those induced by simple microtubule depolymerization.

#### **ACKNOWLEDGEMENTS**

We thank E. Mandelkow for critical reviewing this manuscript. This work was supported by the Max-Planck-Society and the Deutsche Forschungsgemeinschaft.

## MATERIALS AND METHODS

### *Preparation of taxol-stabilized microtubule sample*

Taxol-stabilized microtubules were prepared incubating tubulin (30  $\mu\text{M}$  final concentration) for 20 min in BRB80 buffer, containing 1 mM GTP at 37<sup>0</sup>C followed by the addition of 170  $\mu\text{l}$  of 10  $\mu\text{M}$  taxol in BRB80. Then microtubules were pelleted by ultracentrifugation at 109,000 g (TLA 100 rotor, Optima™ MAX Ultracentrifuge, Beckman) for 5 min, and resuspended in 50  $\mu\text{l}$  BRB80 containing 10  $\mu\text{M}$  taxol (BRB80-taxol). Taxol-stabilized microtubules are always diluted in a taxol-containing buffer.

### *Preparation of GMPCPP microtubule sample*

GMPCPP microtubules were polymerized as described<sup>22</sup> at a tubulin concentration of 10  $\mu\text{M}$  instead of 4  $\mu\text{M}$ .

### *Calcium and MCAK/AMPPNP induced microtubule depolymerization*

Microtubule depolymerization was induced by addition of calcium (40 mM final concentration) or MCAK/AMPPNP (0.2  $\mu\text{M}$  MCAK, 0.5 mM AMPPNP) to the microtubule sample in BRB80 as previously described<sup>3</sup>. Recombinant MCAK was obtained as described<sup>23</sup>. The mixture was deposited on freshly cleaved mica immediately, and left at least 1 minute on the surface before extensive washing with BRB80 buffer.

### *Determining protofilament radius, tubulin distance and kink between tubulin monomers*

We used “Image J” software to fit a circle of a given radius onto bent or ring-like protofilaments. Then we measured the periodicity of the height profile along the protofilament revealing the average distance between tubulin monomers. Both protofilament radius,  $r$ , and average tubulin distance,  $l$ , were used to calculate the kink according to  $kink(^{\circ})=2\pi r/(360\cdot l)$ . By determining the average radius of protofilaments at a certain time after preparing the sample we could then directly relate this time to the progression of the kink.

#### *Sample adsorption to mica and AFM imaging*

Samples were allowed to adsorb to freshly cleaved mica for at least 1 minute followed by rinsing (at least 3 times) with buffer (50 mM HEPES pH 7.4 adjusted with KOH, 200 mM KCl 2 mM MgCl<sub>2</sub> or BRB80). Mixtures of microtubules+40 mM Ca<sup>2+</sup> or microtubules+MCAK were deposited on freshly cleaved mica immediately after preparation, and left 1 minute for adsorption before extensively washing with BRB80 or HEPES buffer. AFM (Nanoscope III, Veeco) imaging was performed in buffer solution using tapping mode. The AFM cantilevers (NPS-oxide sharpened silicon nitride probes (Veeco) exhibiting spring constants of 0.32 or 0.58 N/m) were activated at their resonance frequencies ranging from 8.5 to 9.5 kHz. For the feedback controls, typical values of setpoint for imaging were between 0.5 to 1.5 V, depending on the drive amplitude. The oscillation amplitude was maintained at 5-10 nm for protofilament imaging.

**REFERENCES**

1. Drake, B., Prater, C.B., Weisenhorn, A.L. Gould, S.A.C., Albrecht, T.R., Quate, C.F., Cannell, D.S., Hansma, H.G. and Hansma, P.K. (1989) Imaging crystals, polymers, and processes in water with the atomic force microscope. *Science*, **243**, 1586-1588.
2. Engel, A. and Muller, D.J. (2000) Observing single biomolecules at work with the atomic force microscope. *Nat Struct Biol*, **7**, 715-718.
3. Müller-Reichert, T., Chretien, D., Severin, F. and Hyman, A.A. (1998) Structural changes at microtubule ends accompanying GTP hydrolysis: information from a slowly hydrolyzable analogue of GTP, guanylyl (alpha,beta)methylenediphosphonate. *Proc Natl Acad Sci U S A*, **95**, 3661-3666.
4. Wang, H.W. and Nogales, E. (2005) Nucleotide-dependent bending flexibility of tubulin regulates microtubule assembly. *Nature*, **435**, 911-915.
5. Melki, R., Fievez, S., and Carlier, M. F. (1996) Continuous monitoring of Pi release following nucleotide hydrolysis in actin or tubulin assembly using 2-amino-6-mercapto-7-methylpurine ribonucleoside and purine-nucleoside phosphorylase as an enzyme-linked assay. *Biochemistry* **35**, 12038-12045.
6. Schiff, P. B., Fant, J., and Horwitz, S.B. (1979). Promotion of microtubule assembly in vitro by taxol. *Nature*, **277**, 665-667.
7. Arnal, I. and Wade, R.H. (1995) How does taxol stabilize microtubules? *Curr Biol*, **5**, 900-908.
8. Zhu, J., Hartman, J., Case, R., Rice, S., and Vale, R. In vitro Studies of Microtubule Structures Using the MAC Mode TM AFM. *Molecular Imaging Corporation Application Notes*. [http://www.molec.com/media/PDFs/B-Biology\\_App\\_notes/B3-Microtubule.pdf](http://www.molec.com/media/PDFs/B-Biology_App_notes/B3-Microtubule.pdf)

9. Xiao, H., Verdier-Pinard, P., Fernandez-Fuentes, N., Burd, B., Angeletti, R., Fiser, A., Horwitz, S.B., and Orr, G.A. (2006). Insights into the mechanism of microtubule stabilization by Taxol. *Proc Natl Acad Sci U S A*, **103**, 10166-10173.
10. VanBuren, V., L. Cassimeris and D. J. Odde (2005). Mechanochemical model of microtubule structure and self-assembly kinetics. *Biophys J*, **89**, 2911-2926.
11. Mickey, B. and J. Howard (1995). Rigidity of microtubules is increased by stabilizing agents. *J Cell Biol*, **130**, 909-917.
12. Hyman, A.A., Chrétien, D., Arnal, I., and Wade, R.H. (1995) Structural changes accompanying GTP hydrolysis in microtubules: information from a slowly hydrolyzable analogue guanylyl-(alpha,beta)-methylene-diphosphonate. *J Cell Biol*, **128**, 117-125.
13. Nogales E. and Wang H-W. (2006) Structural intermediates in microtubule assembly and disassembly : how and why ?. *Curr Opin Cell Biol*, **18**, 1-6.
14. Amos, L. and Klug, A. (1974) Arrangement of subunits in flagellar microtubules. *J Cell Sci*, **14**, 523-549.
15. Krebs, A., Goldie, K.N. and Hoenger, A. (2005) Structural rearrangements in tubulin following microtubule formation. *EMBO Rep*, **6**, 227-232.
16. Desai, A., Verma, S., Mitchison, T.J. and Walczak, C.E. (1999) Kin I kinesins are microtubule-destabilizing enzymes. *Cell*, **96**, 69-78.
17. Moores, C.A., Yu, M., Guo, J., Beraud, C., Sakowicz, R. and Milligan, R.A. (2002) A mechanism for microtubule depolymerization by KinI kinesins. *Mol Cell*, **9**, 903-909.

18. Niederstrasser, H., Salehi-Had, H., Gan, E.C., Walczak, C. and Nogales, E. (2002) XKCM1 acts on a single protofilament and requires the C terminus of tubulin. *J Mol Biol*, **316**, 817-828.
19. Sorger, P.K., Dobles, M., Tournebize, R., and Hyman, A.A. (1997) Coupling cell division and cell death to microtubule dynamics. *Curr Opin Cell Biol*, **9**, 807-814.
20. Severin FF., Sorger, P.K., and Hyman, A.A. (1997) Kinetochores distinguish GTP from GDP forms of the microtubule lattice. *Nature*, **388**, 888-891.
21. Westermann S, Avila-Sakar A, Wang HW, Niederstrasser H, Wong J, Drubin DG, Nogales E, Barnes G. (2005). Formation of a dynamic kinetochore- microtubule interface through assembly of the Dam1 ring complex. *Mol Cell*, **17**, 277-290.
22. Howard, J. and Hyman, A.A. (1993) Preparation of marked microtubules for the assay of the polarity of microtubule-based motors by fluorescence microscopy. *Methods Cell Biol*, **39**, 105-113.
23. Hunter, A.W., Caplow, M., Coy, D.L., Hancock, W.O., Diez, S., Wordeman, L. and Howard, J. (2003) The kinesin-related protein MCAK is a microtubule depolymerase that forms an ATP-hydrolyzing complex at microtubule ends. *Mol Cell*, **11**, 445-457.

**FIGURE LEGENDS****Figure 1. Conformations of individual tubulin protofilaments imaged by AFM.**

(A) Products of calcium (40 mM) induced GMPCPP microtubules depolymerization. (B) Unstabilized GDP protofilaments imaged quickly after deposition on mica. (C) Individual protofilaments are present in the sample of taxol-stabilized microtubules and present either in straight, curved, and closed or open ring-like conformations. (D) After 2 days of aging, the taxol-stabilized protofilaments present a ring-like conformation, either closed (1), open (2) or even double ring (3). Addition of MCAK/AMPPNP induced ring-like protofilaments from GMPCPP-stabilized microtubules (E) and taxol-stabilized microtubules (F,G). Nevertheless ends of taxol-stabilized microtubules maintain a straight (blunt) conformation (F). (G) Ring-like protofilaments obtained after MCAK addition to taxol-stabilized microtubules (inset shows higher resolution image). (H) MCAK/ATP, unlike MCAK/AMPPNP, does not induce accumulation of ring-like protofilaments. The gray levels of the AFM topographs correspond to vertical scales of 6 nm (A), 10 nm (B,D), 22 nm (C), 20 nm (E,H), 8 nm (G), and 30 nm (F). Scale bars of insets correspond to 20 nm.

**Figure 2. Straight-to-ring transition of tubulin protofilaments.** (A) Gallery presenting the different protofilaments conformations observed from taxol-stabilized microtubules. The gray levels of all AFM topographs correspond to vertical scales of 22 nm. (B) Occurrence of the different structural intermediates depends on sample aging. For each condition imaged by AFM we analyzed about 100 single protofilaments to determine their conformational statistics. Cartoons at the bottom relate

the structural intermediates occurring during the straight-to-ring transition of protofilaments: the straight, slightly curved, highly curved, half-ring, almost-closed and closed ring conformations.

**Figure 3. High-resolution AFM directly observes single tubulin molecules forming protofilaments.** (A) Freshly prepared straight taxol-stabilized protofilaments. (B) The height profile along protofilament sections reveals an average tubulin periodicity of  $4.2 \pm 1.9$  nm ( $n=104$ ). (C) With increasing time taxol-stabilized protofilaments transform into slightly curved conformations. (D) Example of a ring-like taxol-stabilized protofilament observed after 2 days aging of the sample. (E) Average number of tubulin monomers counted per ring-like protofilament corresponds to  $30 \pm 1$  ( $n=10$ ). (F) Kink between tubulin monomers calculated from the radius of curvature of protofilaments observed under different conditions. Red line represents kink over protofilament curvature radius calculated for a subunit size of 4.2 nm. Experimental averages of radii are given for native and for taxol- and GMPCPP-stabilized protofilaments, in absence and in presence of calcium or MCAK. No time given in legend of (F) indicates that the structures were observed roughly 1h after protofilament preparation and immediately after MCAK or calcium addition to protofilaments. The gray levels of all AFM topographs correspond to a vertical scale of 22 nm.

## TABLES

<b>Sample</b>	<b>Protofilament radius of curvature (nm ± SD)</b>
GDP protofilaments	21 ± 4 ( <i>n</i> =45)
GDP protofilaments + 40 mM Ca <sup>2+</sup>	21 ± 2 ( <i>n</i> =56)
GMPCPP protofilaments + 40 mM Ca <sup>2+</sup>	31 ± 5 ( <i>n</i> =35)
GMPCPP protofilaments + MCAK/AMPPNP	27 ± 4 ( <i>n</i> =43)
Taxol-stabilized protofilaments (Fresh)	245 ± 105 ( <i>n</i> =51)
Taxol-stabilized protofilaments + 40 mM Ca <sup>2+</sup>	21 ± 2 ( <i>n</i> =57)
Taxol-stabilized protofilaments (2 days old)	21 ± 2 ( <i>n</i> =48)
Taxol-stabilized protofilaments + MCAK/AMPPNP	19 ± 2 ( <i>n</i> =37)

**Table 1. Radius of curvature of tubulin protofilaments.**

Figure 1  
[Click here to download high resolution image](#)

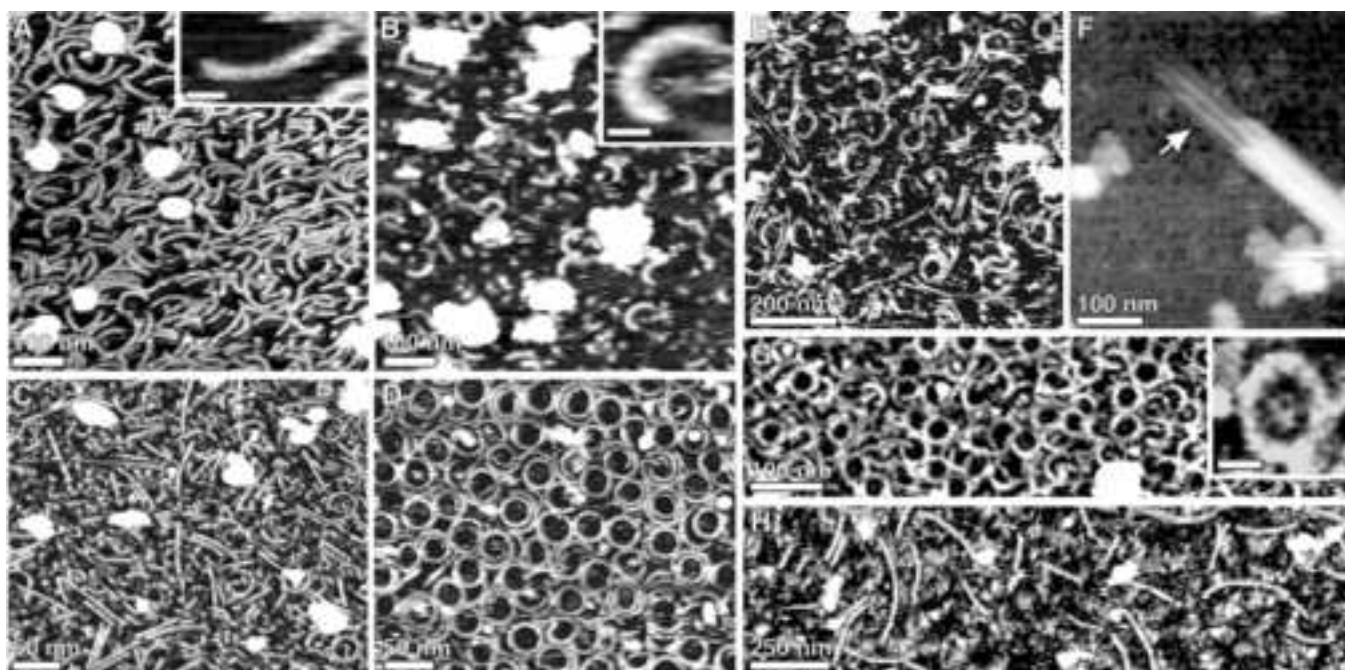
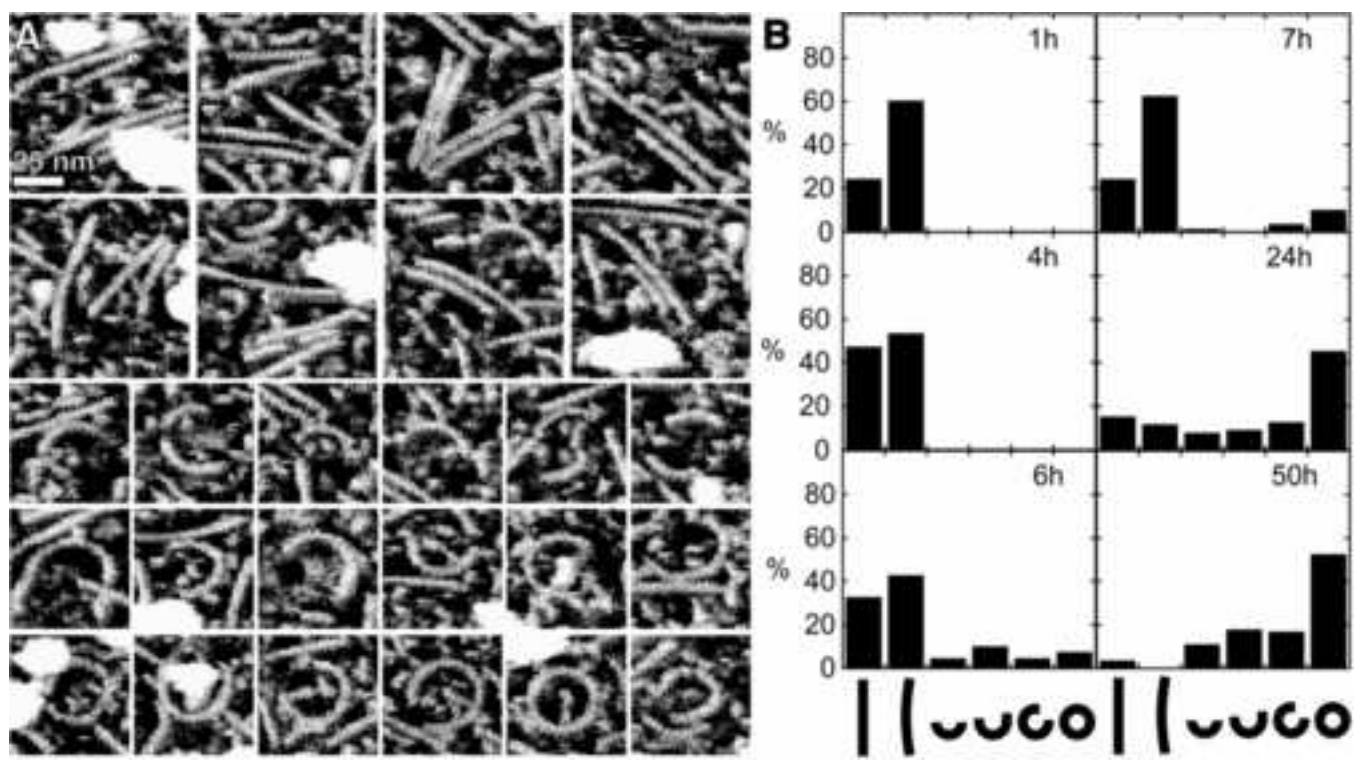
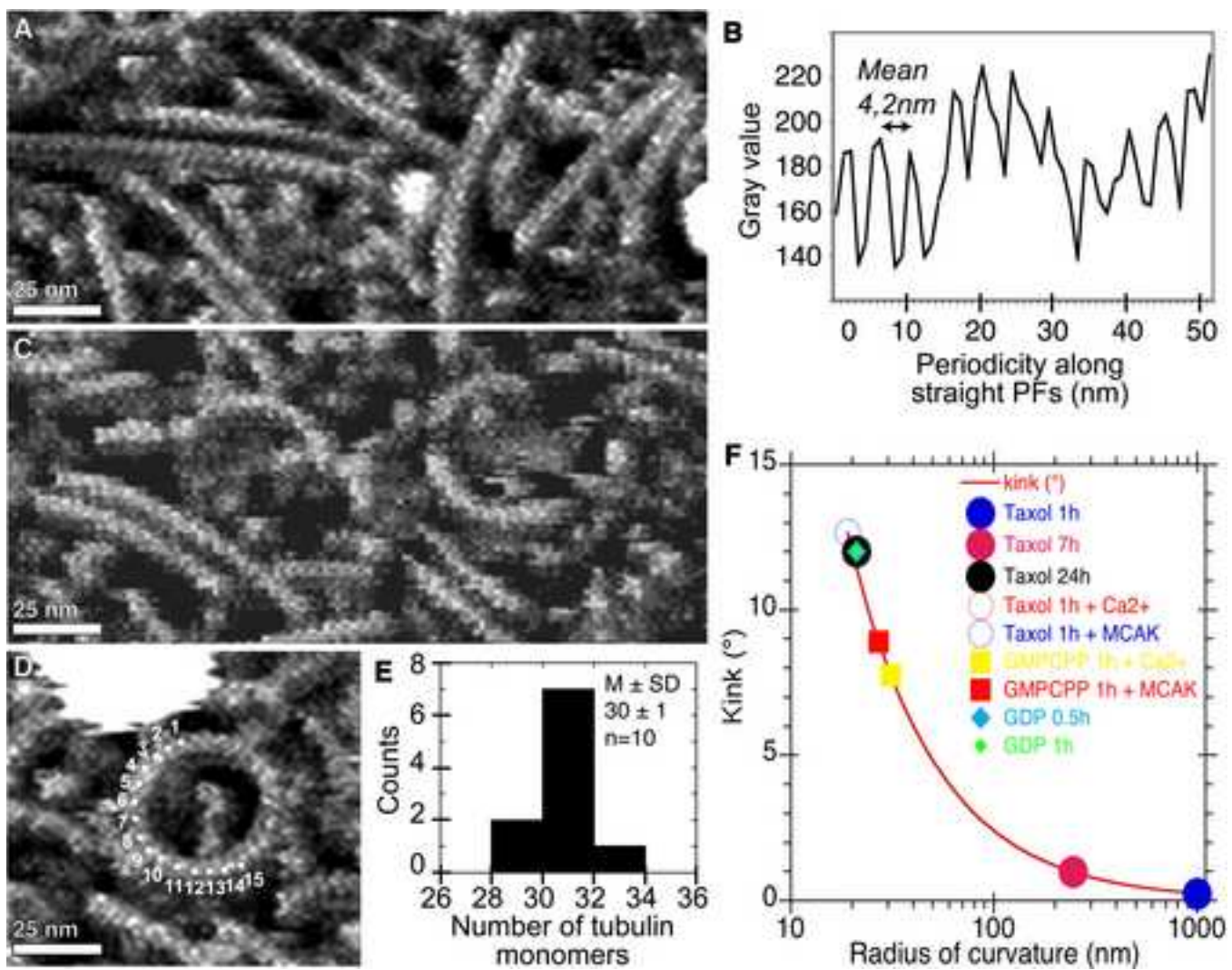


Figure 2  
[Click here to download high resolution image](#)

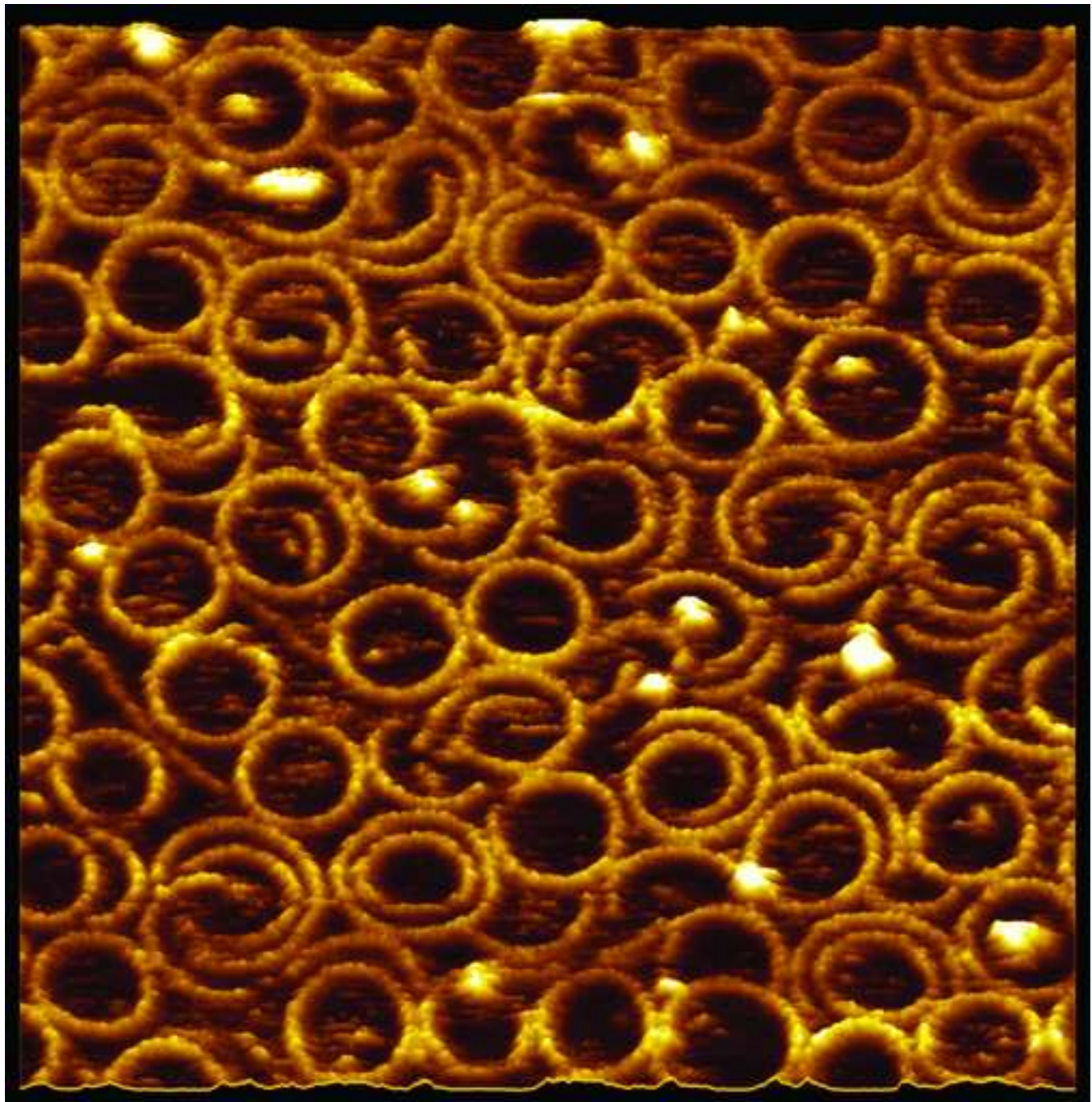


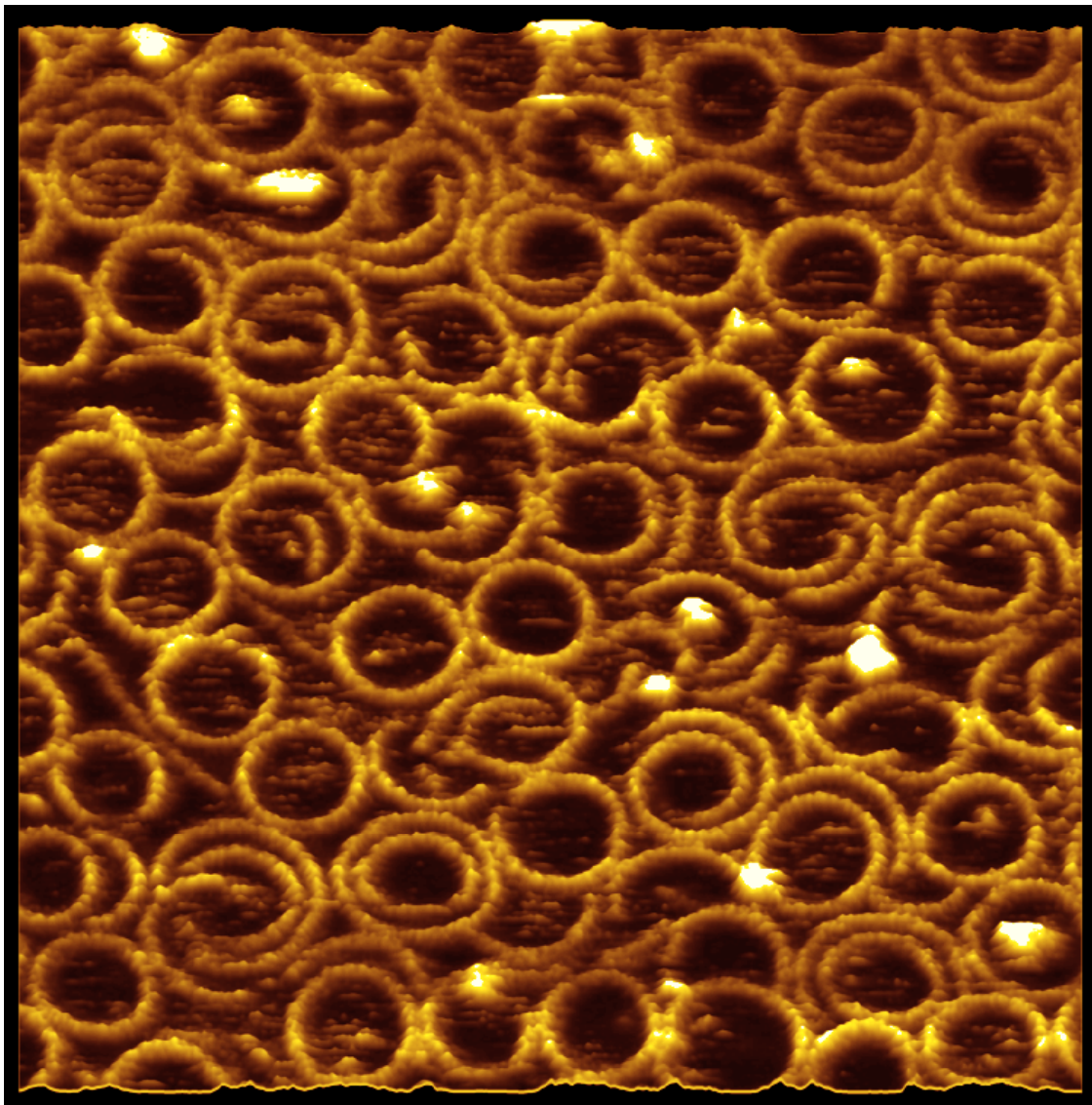
**Figure 3**  
[Click here to download high resolution image](#)



Frontcover suggestion

[Click here to download high resolution image](#)





**Frontcover suggestion – High-resolution AFM of native protofilaments.**

Individual protrusions of the ring-like structures represent tubulin subunits forming protofilaments. The unprocessed AFM topograph (380 x 380 nm) showing native protofilaments (no staining and no fixation) was recorded in buffer solution.